Chinese Chemical Letters 31 (2020) 281–284

Contents lists available at ScienceDirect

Chinese Chemical Letters

journal homepage: www.elsevier.com/locate/cclet

Communication

CO_2/NIR light dual-controlled nanoparticles for dsDNA unzipping

Yanjing Wang[a], Hongbo Yuan[a], Dawei Li[b], Chengfen Xing[a,*]

[a] Key Laboratory of Hebei Province for Molecular Biophysics, Institute of Biophysics, Hebei University of Technology, Tianjin 300401, China
[b] Institute of Polymer Science and Engineering College of Chemical Engineering, Hebei University of Technology, Tianjin 300130, China

ARTICLE INFO

Article history:
Received 14 March 2019
Received in revised form 1 April 2019
Accepted 9 April 2019
Available online 11 April 2019

Keywords:
Carbon dioxide
Conjugated polymers nanoparticles
Photothermal effect
dsDNA
Near-infrared light

ABSTRACT

Both of carbon dioxide (CO_2) and near-infrared (NIR) light as triggers for non-invasive remotely control are attracting wide attentions due to their good biocompatibility and easy operation. Here, CO_2/NIR light dual controlled nanoparticles are proposed to remotely regulate the unzipping of dsDNA by using imidazole functionalized conjugated polymer nanoparticles (imidazole-CPNs). The dsDNA successfully coats on the shell of imidazole-CPNs to form imidazole-CPNs/dsDNA assembly due to intensively electrostatic interaction triggered by CO_2. Furthermore, the unzipping process of dsDNA is remotely controlled by NIR light based on the photothermal effect, and it can be readily monitored by the fluorescence intensity of ethidium bromide (EB) and CD spectra of dsDNA. Thus, dual stimulation responsive imidazole-CPNs effectively control dsDNA unzipping under CO_2 stimulus and NIR light, promising a new direction in the biological applications of DNA, such as the treatments of diseases caused by gene duplication abnormality.

Non-invasive remote control and modulation of biological events are advanced technologies for manipulating physiological process and disease treatment [1]. As a remote controller, near-infrared (NIR) light has been widely employed to regulate cellular activities, because NIR light not only can penetrate into deep tissues but also can be transformed into heat based on the photothermal therapy (PTT) [2,3]. In the past decade, conjugated polymers nanoparticles (CPNs) have been drawing much attention in biosensing, imaging, disease diagnosis and therapy by virtue of their unique advantages including versatile surface functionalization, good water dispersion and biocompatibility, excellent photostability and tunable optoelectronic properties [4–7]. In addition, various CPNs with NIR absorption and emission have been developed by altering the electron donor and electron acceptor (D-A) building blocks in the conjugated polymers for extending their biomedical applications [8]. For example, Wang's group designed a novel strategy to remotely control the gene expression in living cells based on the NIR-active and photothermal-responsive CPNs [9]. Pu and coauthors reported hybrid nanoparticles composed of NIR-absorbing conjugated polymers and nanoceria to serve as the photosensitizer and the ROS regulator to improve the phototherapeutic performance in cancer therapy [10].

Carbon dioxide (CO_2), as a "green" trigger, has been extensively used in development of stimuli-responsive polymers [11], because of its energy-efficient characteristics and good biocompatibility compared to other stimuli including pH, redox agents, ions and magnetic fields [12–14]. The structure and properties of CO_2 stimuli-responsive polymers will readily change after reacting with CO_2 based on the CO_2 stimuli-responsive groups, such as amidine, amine or carboxyl, resulting in a wide applicability both in CO_2-controlled assembly and biomimetic materials [15,16]. For example, our group reported several CO_2 stimuli-responsive conjugated polymers for CO_2 sensing [17–19] and fabrication of CO_2 responsive biomimetic supramolecular assembly [20]. Jessop's group developed a library of CO_2 controlled on–off switches including solvents, solutes and surfactants based on functionalization of the materials with amidine moieties [21]. Yuan and coauthors designed the amphiphilic diblock copolymer containing amidine groups, which formed "breathing" vesicles in aqueous solution with reversible size controlled by introducing and removing CO_2 [22]. In addition, oligonucleotides such as single-stranded DNA (ssDNA) are widely explored in gene therapy to replace a defective gene or to inactivate a harmful gene product [23]. Because nucleic acids macromolecules are usually hindered by biomembrane and easily degraded by enzymes in cell [24], many strategies are developed by assembling DNA with functionalized nanoparticles, which can efficiently penetrate cell membrane and release DNA in cells based on the photothermal effect [25,26]. However, most of the nanoparticles used in gene delivery

* Corresponding author.
E-mail address: xingc@hebut.edu.cn (C. Xing).

https://doi.org/10.1016/j.cclet.2019.04.020
1001-8417/

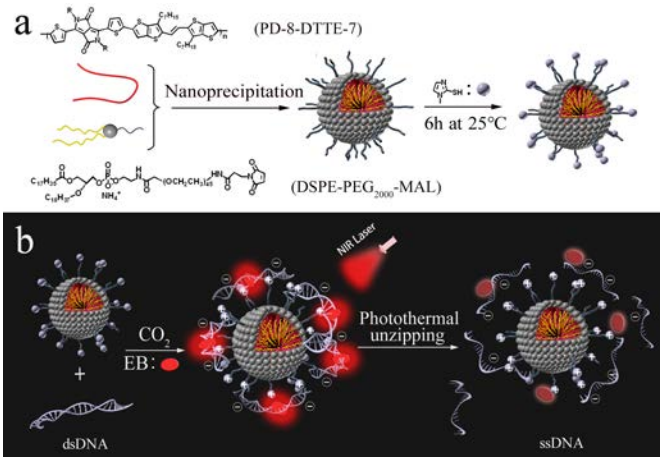

Scheme 1. (a) Schematic illustration of the preparation of imidazole-CPNs. (b) Schematic representation of dsDNA unzipping regulated by imidazole-CPNs in the presence of CO_2 under NIR light.

systems are controlled by single cue [27,28], which limits its application in the complicated environment of cell. Therefore, inspired by these observations, we fabricate CO_2/NIR dual controlled CPNs to manipulate the biological process.

Here, an imidazole functionalized conjugated polymers nanoparticles (imidazole-CPNs) is fabricated to remotely unzip dsDNA under CO_2 stimulus and NIR light. As shown is Scheme 1, 1,2-distearoyl-sn-glycero-3-phosphor-ethanol-amine-*N*-[maleimide-(polyethyleneglycol)-2000] (DSPE-PEG_{2000}-Mal) is used as the encapsulation matrix. The imidazole-CPNs were prepared by using nanoprecipitation method through coprecipitating donor-acceptor (D-A) type conjugated polymer (PD-8-DTTE-7) with DSPE-PEG_{2000}-Mal. Furthermore, the imidazole groups are grafted on the shell to endow the CPNs with CO_2 responsive features. Upon reacting with CO_2, the imidazole groups are protonated and the nanoparticles exhibit positive charges, leading to dsDNA absorption on to the surface of CPNs showing strong fluorescence of ethidium bromide (EB), based on the intensive electrostatic interaction. And then, the dsDNA is unzipped into ssDNA under NIR irradiation based on the photothermal effect of PD-8-DTTE-7 which disrupts the hydrogen bonds between base pairs and separate double stranded helix into two single strands by heat, resulting in releasing of EB and the quenching of the fluorescence. However, dsDNA is unable to assemble with imidazole-CPNs in the absence of CO_2, or unzipped without NIR irradiation. Compared with traditional approaches for unzipping dsDNA including heating, force or chemical denaturants, both of NIR light and CO_2 are biocompatible, and can freely penetrate into cell membrane [29–31]. Therefore, CO_2/NIR dual controlled CPNs with two biocompatible transducers exhibit promising applications in remote manipulation of biological event.

In order to analyze the ability of imidazole-CPNs to remotely control the unzipping process of dsDNA under NIR irradiation in the presence of CO_2 based on the photothermal effect of PD-8-DTTE-7, we employed ethidium bromide (EB) as a probe which contains a planar structure that can intercalate into the double helix strands of dsDNA with strong flurescence emission. As shown in Fig. 1a, EB probe exhibited very strong fluorescence intensity before NIR irradiation. However, 86.5% of the emission intensity of EB was quenched after 808 nm laser irradiation with the power density of 2.0 W/cm^2 for 2.5 min, thanks to the transformation of dsDNA to ssDNA. This indicates that dsDNA was absorbed on the shell of imidazole-CPNs in the presence of CO_2 due to the strong electrostatic interaction, and then it was unwound into single-stranded DNA leading to releasing of EB based on the photothermal effect of imidazole-CPNs under NIR irradiation, which is consistent with the working mechanism proposed in Scheme 1. However, control experiments demonstrated that dsDNA could not strongly interact with imidazole-CPNs without CO_2-stimuli resulting in the weak modulation activity (Figs. S1 and S2 in Supporting information). In addition, the fluorescence intensity of EB gradually decreased with the increasing NIR illumination time, indicating that more and more dsDNA transformed into ssDNA induced by NIR (Fig. 1b). To further confirm the unzipping of dsDNA controlled by CO_2/NIR, circular dichroism (CD) spectroscopy was employed to measure the conformational changes of dsDNA. For the dsDNA, CD spectra exhibit a positive peak at 256 nm and a negative at 248 nm which are the characteristic signals of right-handed double helix of the B-type dsDNA [32]. Upon treating with CO_2/NIR, however, CD spectra exhibited the weakness of the peak at 256 nm and the appearance of positive peaks at 248 nm, which are the characteristic signals of ssDNA (Fig. 1c). Moreover, agarose gel electrophoresis experiments were performed to further proof the dsDNA unzipping activity of imidazole-CPNs under CO_2/NIR. As shown in Fig. 1d, only a 20 base pairs band was observed before NIR irradiation that identifies with dsDNA. However, a new ssDNA band of 20 bases clearly emerged after illumination, which is the direct evidence of the transformation of dsDNA into ssDNA. Therefore, these results illustrate that the unzipping of dsDNA can be remotely controlled by CO_2 stimuli and NIR irradiation based on the imidazole-CPNs.

Taking the photothermal effect of PD-8-DTTE-7 in to consideration, the photothermal performance of imidazole-CPNs was further investigated. As demonstrated in Fig. 2a, infrared thermal images of imidazole-CPNs aqueous solution with various

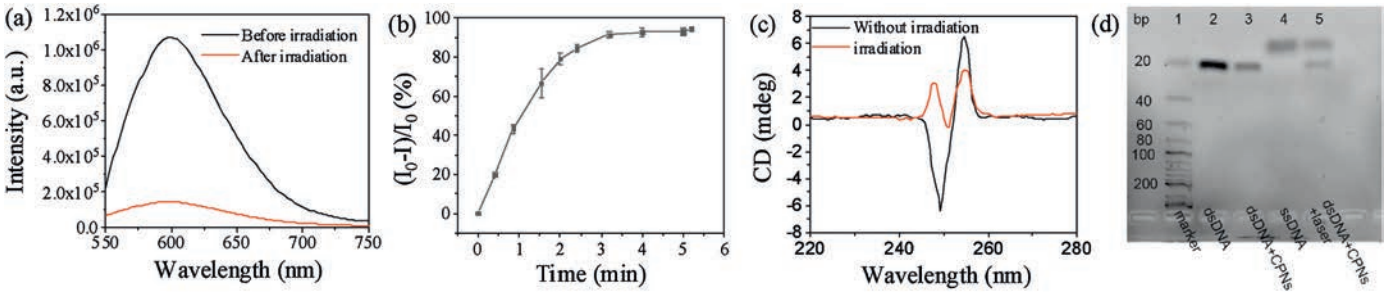

Fig. 1. (a) Fluorescence spectra of the EB with dsDNA and imidazole-CPNs in the presence of CO_2 before and after 808 nm NIR laser irradiation for 2.5 min. The power density was 2.0 W/cm^2. (b) Fluorescence intensity of EB with dsDNA and imidazole-CPNs in the presence of CO_2 as a function of NIR irradiation time. I_0 indicates the fluorescence intensity of EB without irradiation and I indicates the fluorescence intensity of EB with irradiation. The excitation wavelength of EB was 485 nm. Error bars were calculated as standard deviations of data from three separate measurements. [dsDNA] = 0.27 μmol/L, [EB] = 0.70 μg/mL, [imidazole-CPNs] = 15.0 μg/mL. (c) CD spectra of dsDNA before and after NIR irradiation in the presence of imidazole-CPNs and CO_2. [dsDNA] = 0.27 μmol/L, [imidazole-CPNs] = 15.0 μg/mL. (d) Agarose gel electrophoresis (4%) analysis of dsDNA before and after NIR irradiation in the presence of imidazole-CPNs and CO_2. [dsDNA] = 0.20 μmol/L, [imidazole-CPNs] = 15.0 μg/mL, [ssDNA] = 0.30 μmol/L.

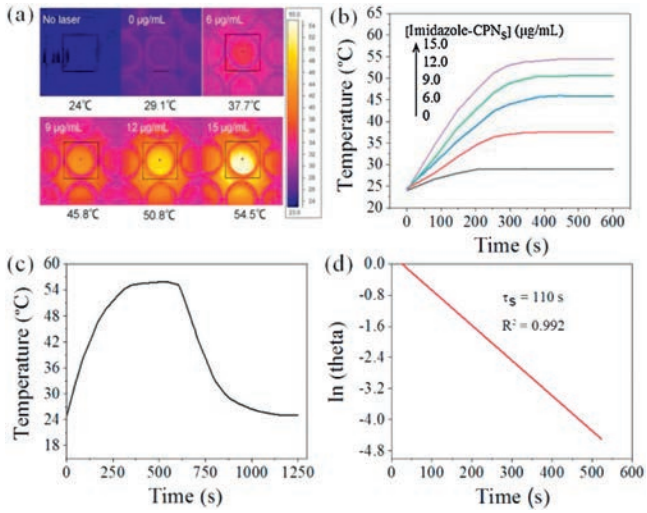

Fig. 2. (a) Infrared thermal images of imidazole-CPNs aqueous solution with various concentrations exposed to 808 nm laser irradiation for 10 min. (b) Temperature profiles of imidazole-CPNs aqueous solution with various concentrations versus irradiation time. The power density was 2.0 W/cm^2. (c) Temperature elevation of imidazole-CPNs (15.0 μg/mL) under 808 nm irradiation (2.0 W/cm^2, 600 s), followed by subsequent cooling to room temperature. (d) Time constant for heat transfer was determined to be τ_s = 110 s by applying the linear time data from the cooling period (after 600 s) *versus* negative natural logarithm of driving force temperature, which is obtained from the cooling stage of (c).

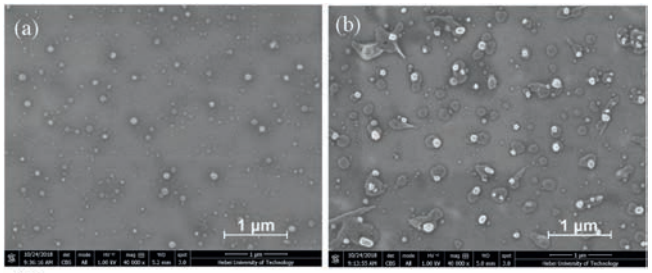

(c)

Nanoparticles	ζ potential (mV)
CPNs	-14.6 ± 0.31
Imidazole-CPNs	-16.8 ± 0.53
Imidazole-CPNs/CO_2	+0.8 ± 0.47
Imidazole-CPNs/CO_2/dsDNA	-3.8 ± 0.27

Fig. 3. The effect of CO_2 on imidazole-CPNs. (a) SEM images of imidazole-CPNs in the presence of CO_2. (b) SEM images of assemblies of dsDNA and imidazole-CPNs in the presence of CO_2. The scale bar was 1 μm. (c) ζ potentials of CPNs, imidazole-CPNs and imidazole-CPNs with CO_2 in aqueous solution.

concentrations under NIR irradiation were captured by infrared thermal camera, revealed that the temperature gradually increased with the increasing amount of imidazole-CPNs after exposing to 808 nm laser irradiation with the power density of 2.0 W/cm^2 for 10 min. The temperature of imidazole-CPNs aqueous solution with concentrations of 15.0 μg/mL reached to 54.5 °C, which is much higher than the melting temperature of dsDNA (42.4 °C) used in this work (Fig. S3 in Supporting information). In addition, the time sweep demonstrated that the temperature increased sharply and reached plateau in 5 min (Fig. 2b). Furthermore, the photothermal conversion efficiency of imidazole-CPNs was calculated. As shown in Fig. 2c, the temperature of imidazole-CPNs (15.0 μg/mL) raised rapidly from 0 s to 300 s under NIR irradiation and reached steady state. Subsequently, NIR laser illuminator was switched off, and the temperature spontaneously decreased to room temperature at 1200 s. The time constant was measured according to the rate of heat transfer from the imidazole-CPNs solution to the environment (Fig. 2d). Finally, the photothermal conversion efficiency of imidazole-CPNs was calculated to be 27.5%. These results show that the imidazole-CPNs can efficiently convert near infrared light energy into heat energy.

To prove the CO_2 triggered assembly between dsDNA and imidazole-CPNs, scanning electron microscopy (SEM) measurements were performed to visualize the morphology of particles. As shown in Figs. 3a and b, imidazole-CPNs form well-dispersed nanoparticles, however, dsDNA intensively assembles with imidazole-CPNs to form supramolecular structure with bigger size upon CO_2-bubbling. It means that dsDNA was substantially absorbed on the shell of imidazole-CPNs based on the electrostatic interaction. In addition, control experiments indicate that dsDNA only can weakly assemble with imidazole-CPNs in the absence of CO_2 (Fig. S4 in Supporting information). Meanwhile, there was no significant change in the particle size and appearance of imidazole-CPNs before and after reacting with CO_2, which was consistent with the results of dynamic light scattering measurements (Fig. S5 in Supporting information). To further understand the mechanism of CO_2 triggered assembly between dsDNA and imidazole-CPNs, the ζ potentials were measured. As shown in Fig. 3c, both of the ζ potentials of CPNs and CPNs grafted with imidazole groups (imidazole-CPNs) were intensively negative. However, the ζ potentials of imidazole-CPNs became slightly positive after reacting with CO_2, from −16.8 mV to +0.8 mV, leading to the electrostatic interaction between dsDNA and imidazole-CPNs. Consequently, imidazole-CPNs became mildly negative after binding with dsDNA in the presence of CO_2. Therefore, CO_2 can readily control the assembly of dsDNA and imidazole-CPNs based on the charge reversal of imidazole groups.

In summary, we have developed a dual stimulation responsive nanoparticles to remotely unzip dsDNA by using imidazole functionalized CPNs (imidazole-CPNs) as the transducer under CO_2 and NIR light irradiation. Upon introducing CO_2, the surface charge of CPNs changes from negative to positive due to the protonation of imidazole groups, which promotes dsDNA successfully coats on the shell of imidazole-CPNs to form imidazole-CPNs/dsDNA assembly based on intensively electrostatic interaction. Moreover, the D-A type conjugated polymers loaded in imidazole-CPNs endow the nanoparticles with good photothermal conversion capacity under NIR light. Therefore, the imidazole-CPNs/dsDNA assembly effectively generates localized heat to trigger dsDNA unzipping under NIR light irradiation. Owing to the wide dispersion and good biocompatibility of CO_2, the combination of CO_2 stimulus and NIR laser to regulate dsDNA unzipping offers a promising strategy for the development of gene thermotherapy.

Acknowledgments

The authors are grateful for the financial support of the National Natural Science Foundation of China (Nos. 21574037, 21773054 and 51803046), the “100 Talents” Program of Hebei Province, China (No. E2014100004), the Natural Science Foundation of Hebei Province (No. B2017202051), the Program for Top 100 Innovative Talents in Colleges and Universities of Hebei Province (No. SLRC2017028).

Appendix A. Supplementary data

Supplementary data associated with this article can be found, in the online version, at https://doi.org/10.1016/j.cclet.2019.04.020.

References

[1] D. Li, D. Gao, J. Qi, et al., ACS Appl. Bio Mater. 1 (2018) 146–152.
[2] Z.A.I. Mazrad, C.A. Choi, S.H. Kim, et al., J. Mater. Chem. B 5 (2017) 7099–7108.
[3] D. Wu, Y. Shen, J. Chen, et al., Chin. Chem. Lett. 28 (2017) 1979–1982.
[4] L. Feng, C. Zhu, H. Yuan, et al., Chem. Soc. Rev. 42 (2013) 6620–6633.
[5] C.Y. Wang, J.M. Hong, G. Chen, et al., Chin. Chem. Lett. 21 (2010) 179–182.
[6] F.F. Peng, Y. Zhang, N. Gu, Chin. Chem. Lett. 19 (2008) 730–733.
[7] H. Mehrabi, M. Kazemi-Mireki, Chin. Chem. Lett. 22 (2011) 1419–1422.
[8] T. Yang, L. Liu, Y. Deng, et al., Adv. Mater. 29 (2017) 1700487–1700495.
[9] Y. Wang, S. Li, P. Zhang, et al., Adv. Mater. 30 (2018) 1705418–1705422.
[10] H. Zhu, Y. Fang, Q. Miao, et al., ACS Nano 11 (2017) 8998–9009.
[11] W. Zheng, G. Yang, N. Shao, et al., J. Am. Chem. Soc. 139 (2017) 13811–13820.
[12] W.L. Chen, F. Li, Y. Tang, et al., Int. J. Nanomed. 12 (2017) 4241–4256.
[13] X. Jia, Y. Zhang, Y. Zou, et al., Adv. Mater. 30 (2018) 1704490–1704498.
[14] M. Czaun, L. Hevesi, M. Takafuji, et al., Chem. Commun. (2008) 2124–2126.
[15] R.W. Flaig, T.M. Osborn Popp, A.M. Fracaroli, et al., J. Am. Chem. Soc. 139 (2017) 12125–12128.
[16] K. Doré, S.B. Dubus, H.A. Ho, et al., J. Am. Chem. Soc. 126 (2004) 4240–4244.
[17] H. Yuan, C. Xing, Y. Fan, et al., Macromol. Rapid Commun. 38 (2017) 1600726–1600733.
[18] H. Yuan, Y. Fan, C. Xing, et al., Anal. Chem. 88 (2016) 6593–6597.
[19] Y. Fan, C. Xing, H. Yuan, et al., ACS Appl. Mater. Interfaces 9 (2017) 20313–20317.
[20] F. Meng, C. Xing, H. Yuan, et al., Chem. Asian J. 12 (2017) 2962–2966.
[21] Y. Liu, Philip G. Jessop, M. Cunningham, et al., Science 313 (2006) 958–960.
[22] Q. Yan, R. Zhou, C. Fu, et al., Angew. Chem. Int. Ed. 50 (2011) 4923–4927.
[23] L. Poon, W. Zandberg, D. Hsiao, et al., ACS Nano 4 (2010) 6395–6403.
[24] M.C.Peitsch B. Polzar, H. Stephan, et al., EMBO J. 12 (1993) 371–377.
[25] A.M. Derfus, G. von Maltzahn, T.J. Harris, et al., Adv. Mater. 19 (2007) 3932–3936.
[26] A. Barhoumi, R. Huschka, R. Bardhan, et al., Chem. Phys. Lett. 482 (2009) 171–179.
[27] S. Yamashita, H. Fukushima, Y. Akiyama, et al., Bioorg. Med. Chem. 19 (2011) 2130–2135.
[28] J. Kim, J. Kim, C. Jeong, et al., Adv. Drug Deliv. Rev. 98 (2016) 99–112.
[29] L. Rouzina, V.A. Bloomfield, Biophys. J. 80 (2001) 882–893.
[30] A. Ivask, N.H. Voelcker, S.A. Seabrook, et al., Chem. Res. Toxicol. 28 (2015) 1023–1035.
[31] C.H. Lee, C. Danilowicz, R.S. Conroy, et al., J. Phys. Condens. Matter 18 (2006) S205–S213.
[32] M. Vorlickova, I. Kejnovska, K. Bednarova, et al., Chirality 24 (2012) 691–698.